

# We are IntechOpen, the world's leading publisher of Open Access books Built by scientists, for scientists

4,800

Open access books available

122,000

International authors and editors

135M

Downloads

Our authors are among the

154

Countries delivered to

TOP 1%

most cited scientists

12.2%

Contributors from top 500 universities



WEB OF SCIENCE™

Selection of our books indexed in the Book Citation Index  
in Web of Science™ Core Collection (BKCI)

Interested in publishing with us?  
Contact [book.department@intechopen.com](mailto:book.department@intechopen.com)

Numbers displayed above are based on latest data collected.  
For more information visit [www.intechopen.com](http://www.intechopen.com)



## Chapter

# Experimental and Theoretical Investigation on the Shear Behaviour of High Strength Reinforced Concrete Beams Using Digital Image Correlation

*Touhami Tahenni and Thibaut Lecompte*

## Abstract

In this chapter an experimental investigation is carried out on high strength concrete beams without transverse reinforcement and with transverse reinforcement. The beams were tested in bending under two concentrated loads using the technique of digital image correlation. In the test setup, the shear zone which is defined by the area of beam between the support point and the loading point was studied by the camera of high resolution. The Gom-Aramis software was used to record and analyse the numerical images by determination of the deformation of concrete in the compressed zone of the beam, to calculate the opening, the spacing and the length of the diagonal cracks. The experimental shear strength of the beams was compared with the theoretical values predicted by the different design codes, such as the American ACI 318, the British Standard BS 8110, the European Eurocode 2, the New Zealand NZS 3101 and the Indian Standard IS456. The results show that all the design codes underestimate the contribution of high strength concrete to the shear resistance of reinforced concrete beams, and greatly overestimate the contribution of transverse reinforcement. The European Eurocode 2 is the only one among the four code models that gives the best prediction of the ultimate shear strength of high strength concrete.

**Keywords:** beam, high strength concrete, shear capacity, cracking, digital image correlation

## 1. Introduction

The shear behaviour of high strength concrete (HSC) beams is an interest research despite the abundance of literature on the subject. However, the principal of this solicitation remains insufficiently explained because up to now, there are no analytical methods which give in detail the different factors influencing shear capacity of HSC beams. For this reason, a number of empirical models, based on testing reinforced concrete beams, are used by the different design codes throughout the world to determine the shear strength of reinforced concrete beams, particularly in the seismic zone. Moreover, the HSC is considered as a new building

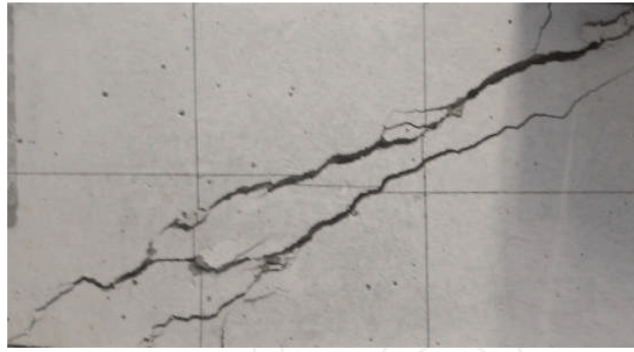


**Figure 1.**  
*Diagonal cracking crossing the aggregates in HSC.*

material, and there is a lack of base data for shear strength of HSC beams, so all the models proposed by the design codes and developed essentially for normal strength concrete (NSC) were extrapolated to HSC, to validate the applicability of these empirical methods to this material. More investigation work is then required to cover this aspect and provide further information.

The present chapter aims to improve the structural behaviour of HSC beams particularly the shear, and thus ameliorate the performance of the built environment to ensure an adequate durability of constructions.

The HSC presents a low resistance under shear [1–3] because the crack surfaces are smooth and cross the aggregates particles as shown in **Figure 1**, which shows a low contribution of the aggregates in the shear strength. However, the HSC is characterised by high compressive strength and by better adhesion with steel reinforcement, which gives a best contributions of the compression zone and the dowel action effect to the shear strength of HSC beams.

## 2. Experimental program

### 2.1 Materials used and concrete mix design

There is no single branded procedure available for mix proportion for HSC, therefore careful selection of the materials is also effective in production of HSC [4]. The ACI 318 [5] defines HSC as concrete with a compressive strength  $>41$  MPa.

The concrete used to prepare the HSC beams is made from the following constituents:

**Cement:** cement used in this work was an Ordinary Portland Cement of type CEM I 52.5 N CE CP2 NF, and was provided by Lafarge group (cement of St-Pierre-la-Cour of Laval in France). The density of this cement is  $3160 \text{ kg/m}^3$  and its specific surface is  $3520 \text{ cm}^2/\text{g}$ , therefore falling within the range of cements that can formulate a HSC (between  $3500$  and  $4000 \text{ cm}^2/\text{g}$ ) [6]. The particle sizes vary between  $0$  and  $100 \text{ }\mu\text{m}$ .

**Fine aggregate:** the sand used to make a HSC must have a modulus of fineness greater than or equal to  $2.8$ . The Sand with a modulus of fineness  $<2.5$  makes the concrete sticky and therefore difficult to compact and less resistant [7]. Rolled sand from the Loire region in France, is used for the present work, with a granular class of  $0/4$  (mm). The fineness modulus of this sand was measured at a value between  $2.9$  and  $3.1$ . This sand also has a water demand of  $<0.5\%$  of its mass.

**Coarse aggregate:** to make the HSC, the ideal granulate must be crushed, cleaned, of regular shape, with a reduced angularity, and containing less flat particles or elongated [8, 9]. Crushed gravel from quartz, with a granular class of  $4/15$

(mm) is used for the present work. This gravel has a water demand of the order of 2–3% of its mass.

**Fine mineral additions:** fine mineral additions consisting of blast furnace slag and limestone fillers. The slag additives were finely ground to give a specific surface of 7000 cm<sup>2</sup>/g and were used in proportion of 10% by weight of cement. This type of addition was provided by Ecocem in France. The fine limestone fillers is Betocarb®HP-EB, manufactured by the Omya-Meac Group in France, and were used in proportion of 23% by weight of cement. The mineral additives were used to fill in the finer gaps between the aggregates and hence to improve the density and the compactness of the concrete material.

**Superplasticizer:** a high range water reducing admixture (HRWRA) in a liquid form, based on polycarboxylates (CHRYSO Fluid Optima 206), was used in a proportion of 2.5% by weight of cement. It is interesting to add the superplasticizer in 1/3 of the quantity with the mixing water to ensure the dispersion of the cement grains, and 2/3 remaining at the end of mixing [10].

**Water:** potable tap water is used.

The mix designs used in making the HSC beams are presented in **Table 1**.

## 2.2 Mechanical properties of concrete

The compressive strengths of HSC used in making the beams without transverse reinforcement and with transverse reinforcement were measured through the crushing tests of cylindrical concrete specimens of 80 mm diameter by 160 mm in height, using a press with capacity of 500 kN. Measurements of the longitudinal compressive strains were carried out with the help of an extensometer (**Figure 2**) and enabled the modulus of elasticity of the HSC. The results were recorded in a data acquisition system (**Figure 3**) for the complete stress-strain curve of HSC (**Figure 4**).

The tensile strength was also evaluated for the HSC by splitting tests of concrete cylinders, 80 mm in diameter and 160 mm in height.

**Figure 4** shows that the pre-peak behaviour is quasi-linear with greater rigidity, and the average ultimate deformation ( $\epsilon_{cu} = 2\%$ ) decreases with the increase in the compressive strength, which is below the ultimate deformation required by the different universal design codes ( $\epsilon_{cu} = 3.5\%$ ) which reflects a decrease in ductility. It should be noted that the HSC specimens exhibit brittle and explosive fracture resulting from a lack of ductility, major disadvantage of this material, as shown in **Figure 2**.

The results of the compressive strength  $f_c$ , the tensile strength  $f_t$  and the modulus of elasticity  $E_c$  of HSC are shown in **Table 2**.

## 2.3 Steel reinforcement

The longitudinal reinforcement composed of two high yield bars of 10 mm diameters in the top zone of the beam (compression), two high yield bars of 8 mm diameters in the bottom zone of the beam (tension) and 6 mm for the transverse reinforcement in the form of stirrups, as shown in **Figures 6(a)** and 7. The steel was

Cement	Slag (10%)*	Limestone filler (23%)*	Gravel	Sand	Water	Admixture (2.5%)*	W/C	Slump test (cm)
382.5	38.25	88.0	1029	700	148.8	9.56	0.38	15

\*By weight of cement.

**Table 1.**  
 Mixing ingredients of HSC (kg/m<sup>3</sup>).

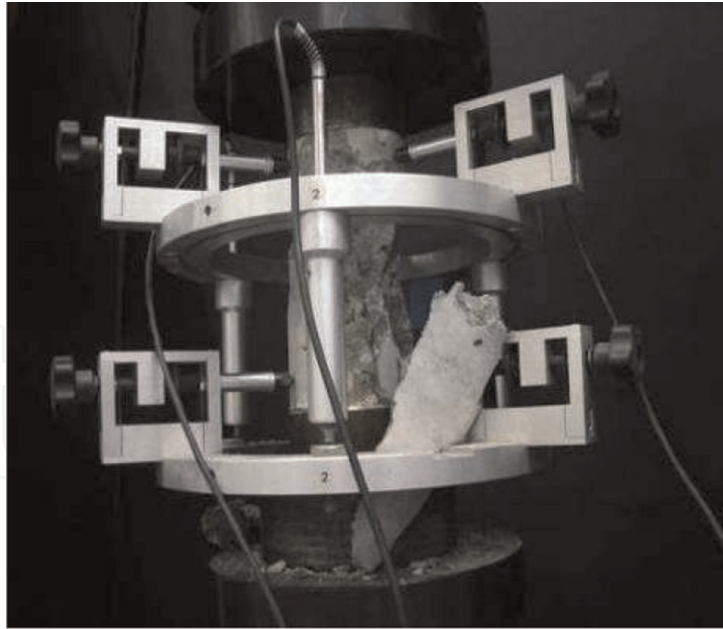


**Figure 2.**  
*Concrete cylinder compression test.*



**Figure 3.**  
*Data acquisition system for the compression test.*

tested under direct tension using a machine with capacity of 500 kN to determine the Young's modulus and the elastic limit. Measurement of the current deformations is carried out by Gom-Aramis software [11] using Digital Image Correlation (DIC) technique (**Figure 5**). The test results give a Young's modulus of 204 GPa and an elastic limit of 500 MPa.

#### **2.4 Beam specimens and testing procedure**

A total of six reinforced HSC beams divided into two series were cast:

- The first series of beams without transverse reinforcement, noted 'Series A'.
- The second series of beams containing transverse reinforcement in the form of stirrups, noted 'Series B'.

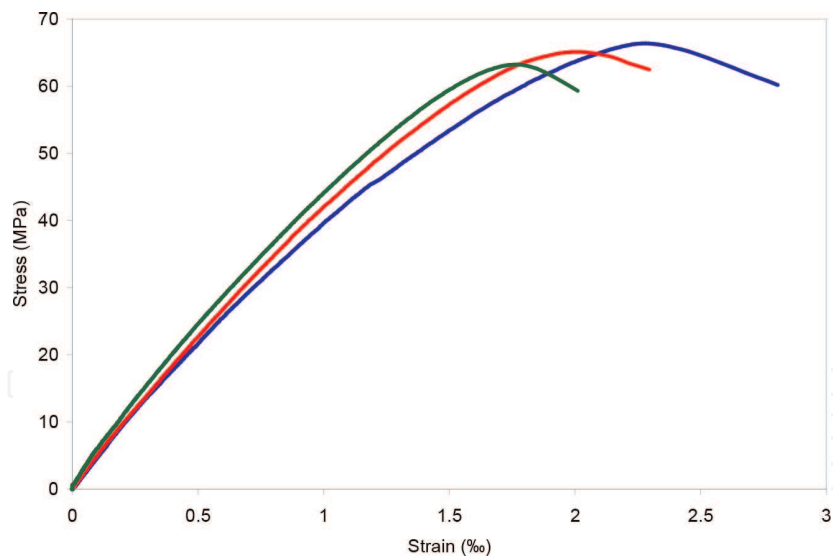


**Figure 4.**  
 Stress-strain curve in compression of HSC.

$f_c$ (MPa)	$E_c$ (GPa)	$f_t$ (MPa)
65 ( $\pm 3$ )	45.2 ( $\pm 5$ )	6 ( $\pm 1$ )

**Table 2.**  
 Average mechanical properties of HSC.

To find a precision in the experimental results, three beams were tested in each series.

The beams were tested under monotonic static loading using a 250 kN servo-controlled hydraulic jack (**Figure 8**). The details of the beams tested are presented in **Table 3**. It is noted that the value of shear-span/effective depth ratio ( $a/d$ ) is within the  $a/d$  ranges leading to a dominant shear behaviour which results in a shear failure of the reinforced concrete beams [6, 12–16].

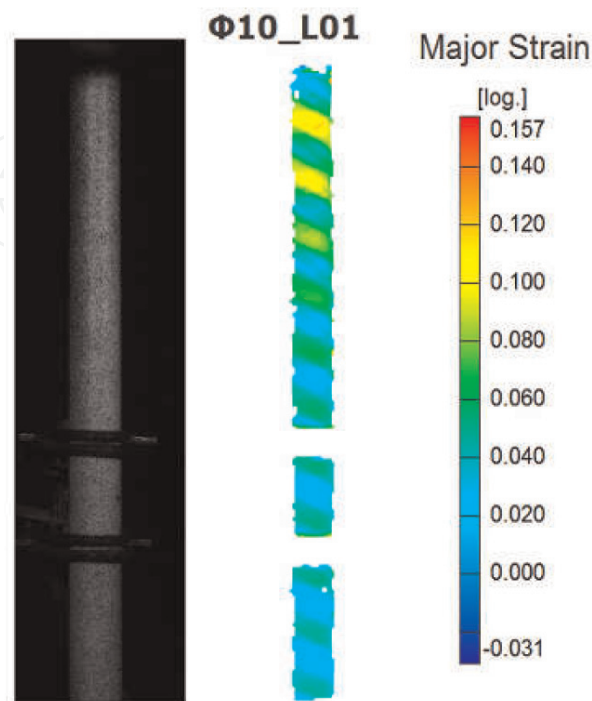


**Figure 5.**  
 Direct tensile test and measurement of the steel deformations by Gom-Aramis software (using DIC).

**Figures 6** and 7 illustrate the casting of the beams and the detail of reinforcement. A highly sensitive video camera was used to detect the development of cracks, monitor the evolution of the diagonal cracks as the load was gradually increased and measure their widths (**Figure 8**). The analysis of the DIC is

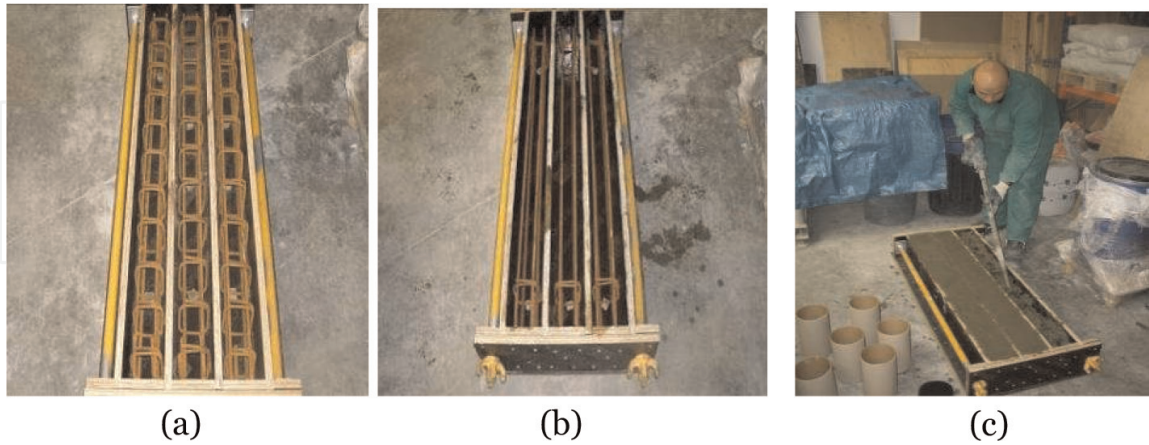


**Figure 6.**  
*Formwork and manufacture of beams. (a) Beams with stirrups, (b) beams without stirrups, and (c) casting of beams.*

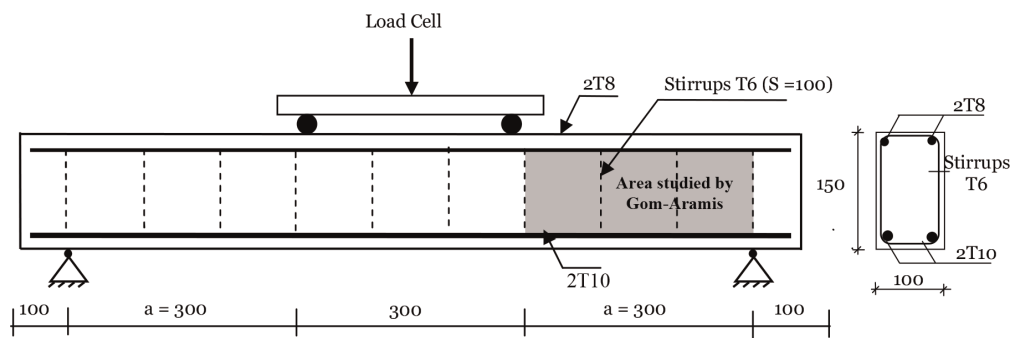


**Figure 7.**  
*Reinforcement of the beam and the flexural device.*

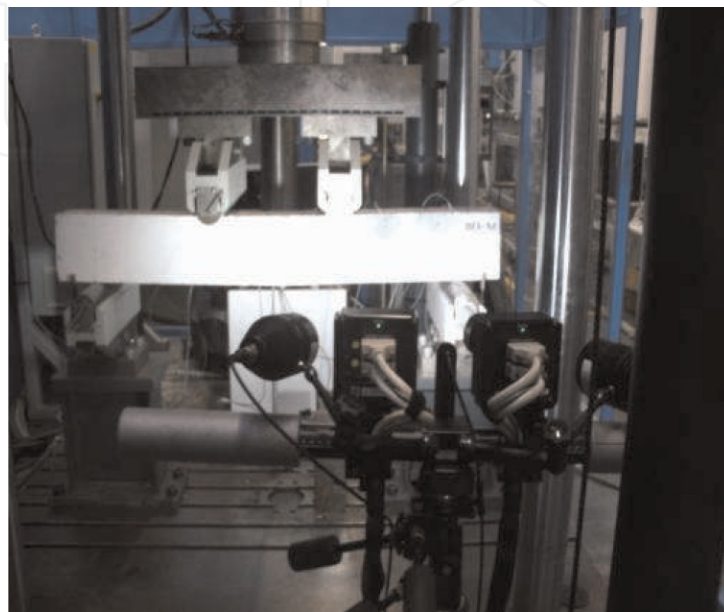


**Figure 8.**  
*Four-point bending test with the camera.*

Identification of beams	b (mm)	h (mm)	d (mm)	a/d	$\rho_s$ (%)	$\rho_w$ (%)	$f_y$ (MPa)
Series A	100	150	135	2.2	1.16	0.00	500
Series B	100	150	129	2.3	1.16	0.56	500

$b$  = width of beam;  $h$  = height of beam;  $a/d$  = shear-span/effective depth;  $\rho_s$  = longitudinal reinforcement ratio;  $\rho_w$  = transverse reinforcement ratio;  $f_y$  = yield strength of longitudinal reinforcement.

**Table 3.**  
Details of the tested beams.

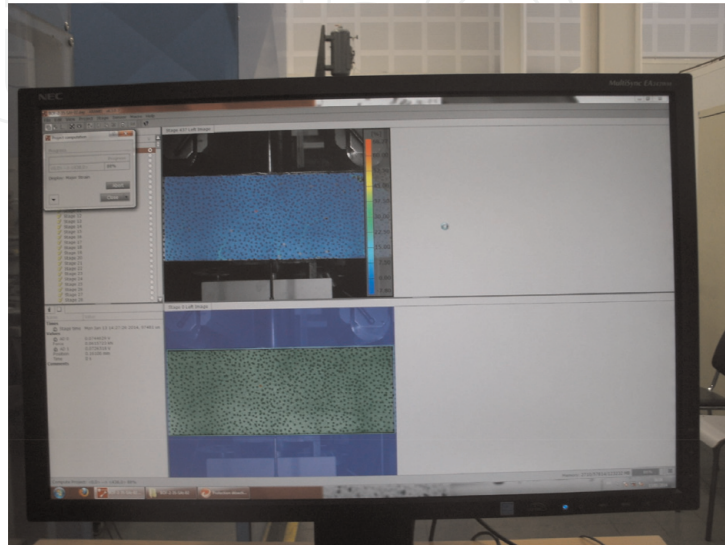


**Figure 9.**  
Image analysis by Gom-Aramis software.

performed by Gom-Aramis software [11] (**Figure 9**) to obtain the deformation of concrete and to monitor the crack evolution in terms of width, spacing and length.

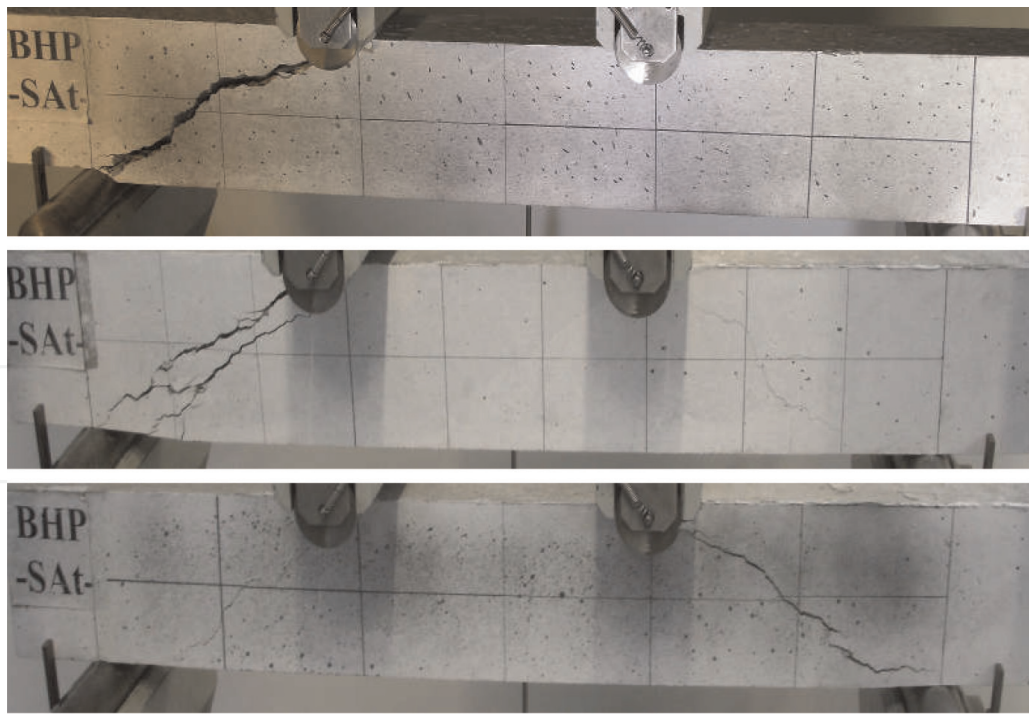
### 3. Analysis of results

#### 3.1 Development of cracks and failure modes of the beams

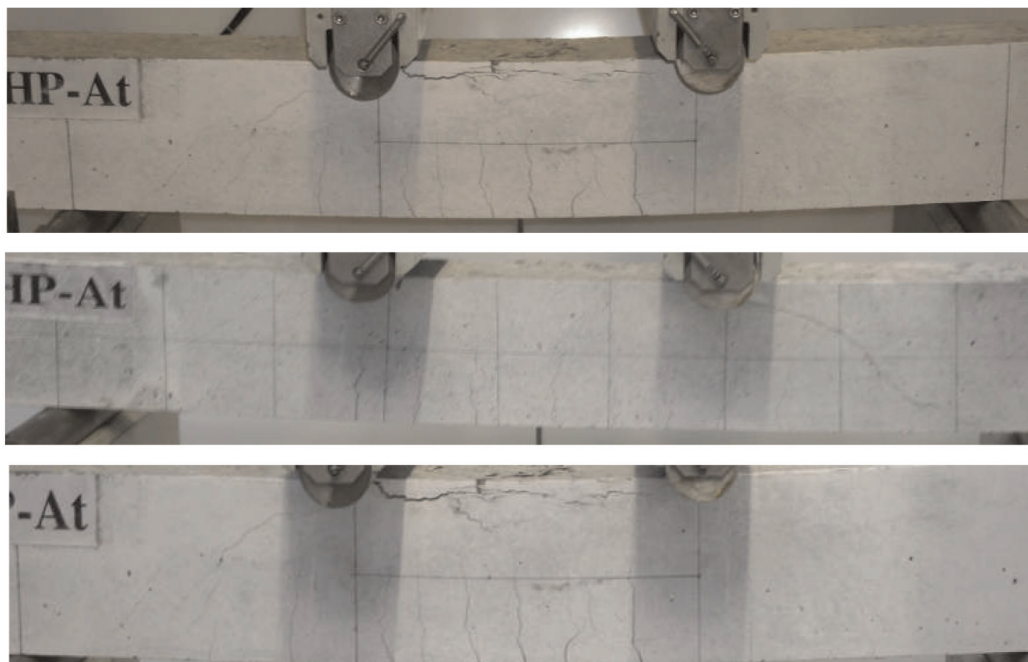
The vertical flexural cracks are the first type developed in the bottom zone of beam between the two point landings; this is the tension zone. The effect of stirrups is considered negligible before the formation of the diagonal cracking. From a loading rang of 60–70% of total ultimate load, the diagonal crackling is occurred from the flexural cracks (**Figure 11(b)**) within the shear zone between the support of the beam and the loading point (**Figure 10(b)**). In the Series A of the beams, the diagonal cracking formed independently of flexural cracks. When this cracking presents a sufficiently width, the failure was also by diagonal cracking as shown in **Figure 10(a)**. This mode of failure is designated by shear.

The addition of the transverse reinforcement in the Series B of the beams retards the appearance of the diagonal cracking and limits their opening and therefore prevents the shear failure of the beam and changes the failure mode of the beam, from shear to flexure. When the diagonal cracking is sufficiently penetrated in the compression zone between the two loading points, the concrete is crushed as shown in **Figure 10(b)**. This mode of failure is designated by shear-compression. This series of beams showed no cracking along the longitudinal reinforcements and have developed many diagonal cracks. Generally, the diagonal cracking is inclined of about 45° with the longitudinal axis of the beam as shown in **Figures 10(a)** and **11(d)**.





(a)



(b)

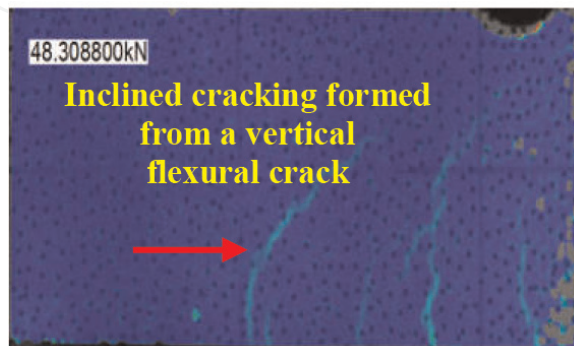
**Figure 10.** Cracks and failure patterns of beams. (a) Failure of Series A (HSC beams without transverse reinforcement) and (b) failure of Series B (HSC beams with transverse reinforcement).

**Table 4** gives the average experimental results of the first crack loads ( $P_{cr}$ ), the diagonal cracking loads ( $P_d$ ) and the total ultimate loads ( $P_u$ ) for all tested beams. The presence of the transverse reinforcements improves the resistance reserve of the beams beyond the diagonal cracking. An increase in the ultimate load varies of around 50% has been recorded for the Series B by comparison to Series A. Comparable results have been reported in the literature [12–15] on reinforced concrete beams made of different strength of concrete ranging from 20 to 68 MPa. This shows that the effect of the transverse reinforcement is practically the same in any type of concrete.

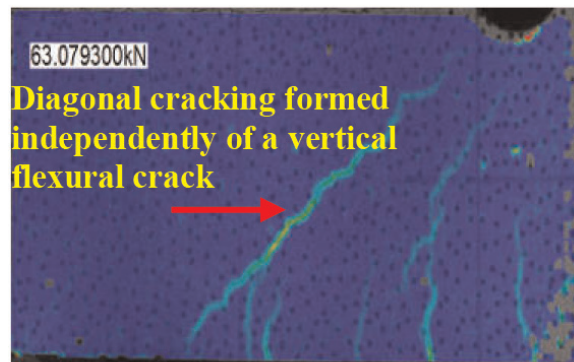
A typical monitoring of a diagonal cracking using DIC is shown in **Figure 11**.



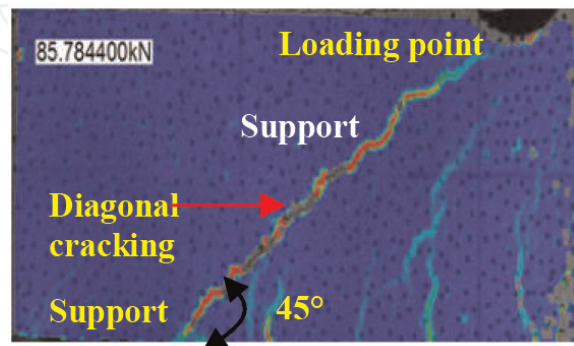
(a)



(b)



(c)



(d)

**Figure 11.** A sequence of crack development within a shear zone in Series B (photos obtained by digitizing video Gom-Aramis). (a) At 24% of ultimate load—no cracking in the shear zone. (b) At 60% of ultimate load—inclined cracking (width = 0.01 mm). (c) At 70% of ultimate load—diagonal cracking (width = 0.04 mm). (d) Just prior to failure—diagonal cracking (width = 0.16 mm).

Identification of beams	$P_f$ (kN)	$P_d$ (kN)	$P_u$ (kN)	Mode of failure
Series A	16.50	43.79	60.00	Shear
Series B	18.75	60.62	86.18	Flexion shear-compression

**Table 4.**  
Diagonal cracking load and ultimate load of the tested beams.

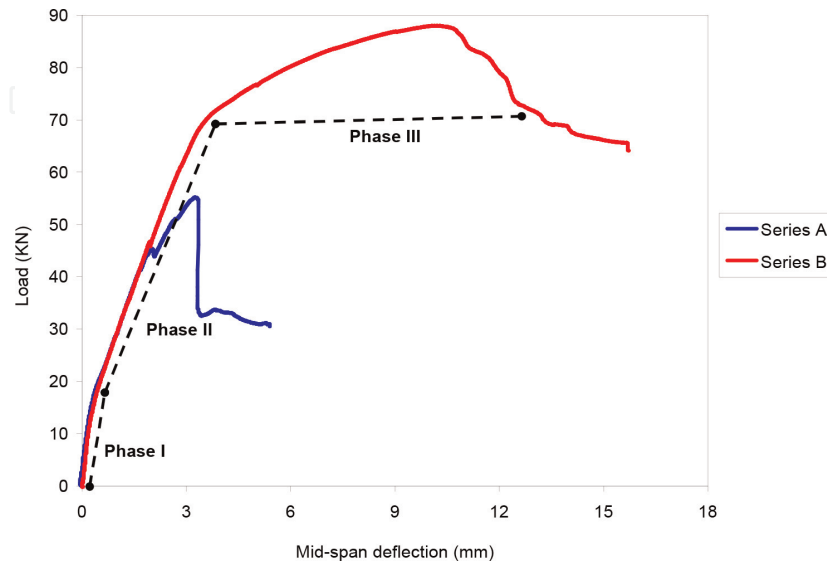


**Figure 12.**  
Load-deflection curves for the HSC beams.

### 3.2 Load-deflection characteristics

One LVDT was attached to the bottom surface of the beams at mid-span to measure the deflection. From the load-deflection curves (**Figure 12**), it can be seen that the behaviour of the beams with transverse reinforcement (Series B) shows three main phases:

- **Phase I:** presents a linear form where the deflection increases at the same time as the load; this is the elastic behaviour of the beams up to the appearance of the first flexural crack.
- **Phase II:** a second phase of linear form after the occurrence of the first flexural crack. The deflection increases with the load but with relatively higher values. In this phase, the cracks are sufficiently developed in length and opening, the Series A of the beams (without transverse reinforcement) lose their rigidity and fail without undergoing further sufficient deflection (**Figure 13**) compared to those containing transverse reinforcement (Series B).
- **Phase III:** corresponds to the plastic behaviour of the beams, where the deflection is not proportional to the load with higher deformation of concrete before the failure of the beams. This phase illustrates the ductile behaviour as shown in **Figure 14**.

### 3.3 Shear analysis of HSC beams

#### 3.3.1 Theoretical analyses of the shear force

The ultimate shear force  $V_u$  in 'kN' of reinforced concrete beam is determined by the contribution of the compression zone  $V_{cy}$ , the contribution of the aggregate

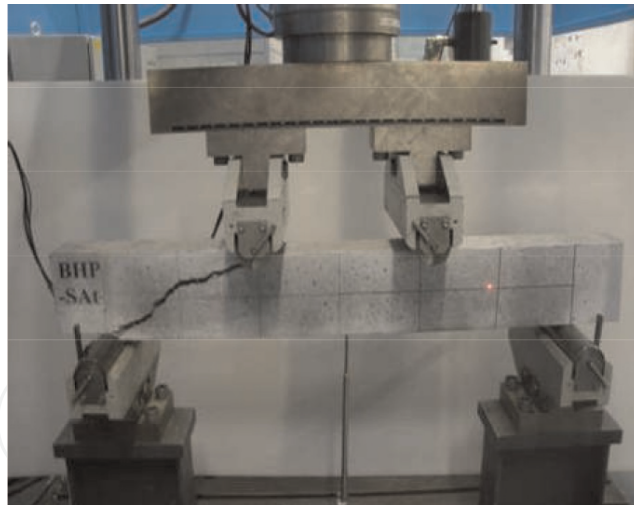


**Figure 13.**  
 Brittle shear failure (Series A).



**Figure 14.**  
 Ductile behaviour (Series B).

interlocking  $V_{ay}$ , the contribution of the longitudinal reinforcement  $V_d$  and the contribution of the stirrups  $V_s$  as shown in Eq. (1) and **Figure 15**. This can be written as:

$$V_u = V_{cy} + V_{ay} + V_d + V_s \quad (1)$$

$(V_{cy} + V_{ay} + V_d)$  expresses the shear resistance of concrete  $V_c$ , and the Eq. (1) is simplified as follows:

$$V_u = V_c + V_s \quad (2)$$

The three shear forces which present the contribution of the concrete to shear strength are evaluated by Taylor [17] and by Paulay and Fenwick [18] as follows:

- $V_{cy} = 20\text{--}40\%$  of  $V_u$
- $V_{ay} = 35\text{--}50\%$  of  $V_u$
- $V_d = 15\text{--}25\%$  of  $V_u$

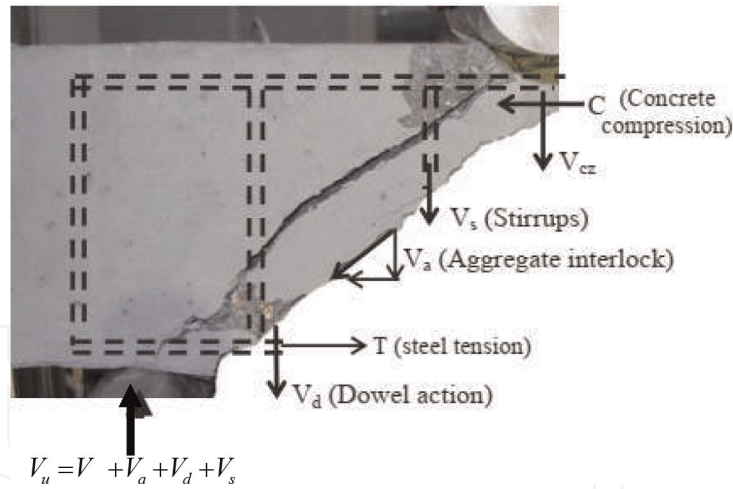


**Figure 15.** Mechanism of shear forces in a beam with transverse reinforcement [15].

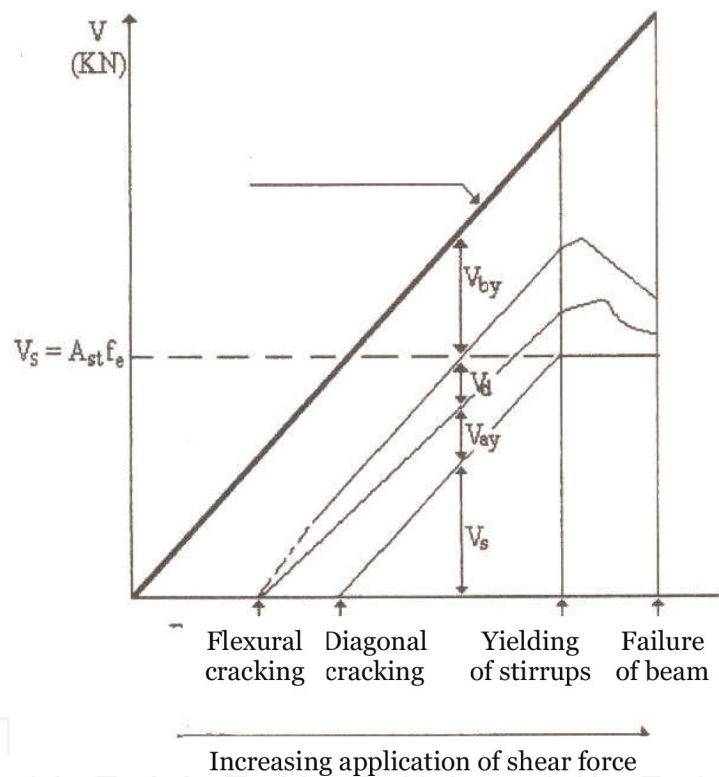


**Figure 16.** Distribution of shear force in a reinforced concrete beams [17].

**Figure 16** shows the contribution of the different components of ultimate shear force ( $V_u$ ) in a reinforced concrete beams as shown in **Figure 14** and given by Eq. (1).

**Table 5** presents the theoretical models to determine the ultimate shear strength of reinforced concrete beams, given by the different universal design codes.

### 3.3.2 Comparison between test results and theoretical predictions of the shear strength

**Figure 17** shows the experimental and the theoretical ultimate shear forces predicted by the five universal design codes presented in **Table 5** above, for two series of beams. The Series A is not transversely reinforced ( $V_s = 0$ ) so the ultimate shear force of this series represents the contribution of concrete to the shear resistance ( $V_c$ ). As shown in this figure, the five models underestimate the contribution

Codes	Model of the total ultimate shear force $V_u$ (kN)	Explanation
ACI 318 [5]	$V_u = \frac{1}{7} (\sqrt{f_c} + 120\rho \frac{d}{a}) b_w d + \frac{A_v f_{sv} d}{s}$	$f_c$ = cylinder compressive strength
BS 8110 [19]	$V_u = \frac{0.79}{\gamma_m} (100\rho)^{\frac{1}{3}} (\frac{400}{d})^{\frac{1}{4}} (\frac{f_{cu}}{25})^{\frac{1}{3}} b_w d + 0.87 \frac{A_v f_{sv} d}{s}$ for $a/d \geq 2$ $V_u = (2\frac{d}{a})^{\frac{0.79}{\gamma_m}} (100\rho)^{\frac{1}{3}} (\frac{400}{d})^{\frac{1}{4}} (\frac{f_{cu}}{25})^{\frac{1}{3}} b_w d + 0.87 \frac{A_v f_{sv} d}{s}$ for $a/d < 2$	$f_{ck}$ = characteristic compressive strength = $f_c/0.8$ $d$ = effective depth of beam $a$ = shear span $b_w$ = width of beam $A_v$ = section of stirrup $f_{sv}$ = yield strength of stirrups
Eurocode 2 [20]	$V_u = 0.18 [k \cdot (100 \cdot \rho \cdot f_c)^{\frac{1}{3}}] b_w d + \frac{A_v f_{sv} z (\cot \theta + \cot \alpha)}{s} \sin \alpha$	$s$ = stirrups spacing $\rho = A_s/b_w d$ $A_s$ = section of longitudinal reinforcement
NZS 3101 [21]	$V_u = (0.07 + 10\rho) \sqrt{f_c} b_w d + \frac{A_v f_{sv} d}{s}$	$f_{cu}$ = cube compressive strength
Indian Standard IS456 [22]	$V_u = \frac{0.85 \sqrt{0.8 f_{ck}} (\sqrt{1+5\beta}-1)}{6\beta} b_w d + \frac{A_v f_{sv} d}{s}$ where $\beta = \frac{0.8 f_{ck}}{6.89(100\rho)} > 1$	$\gamma_m$ = material partial safety factor for shear, taken as 1.25 $\alpha$ = inclination of stirrups ( $\alpha = 90^\circ$ ) $\theta$ = angle between inclined concrete struts and the main tension chord ( $\theta = 45^\circ$ ) $k = 1 + \sqrt{\frac{200}{d}}$ , $d$ (mm) $z$ = lever arm = $0.9d$

**Table 5.** Theoretical models of the ultimate shear strength given by different codes.

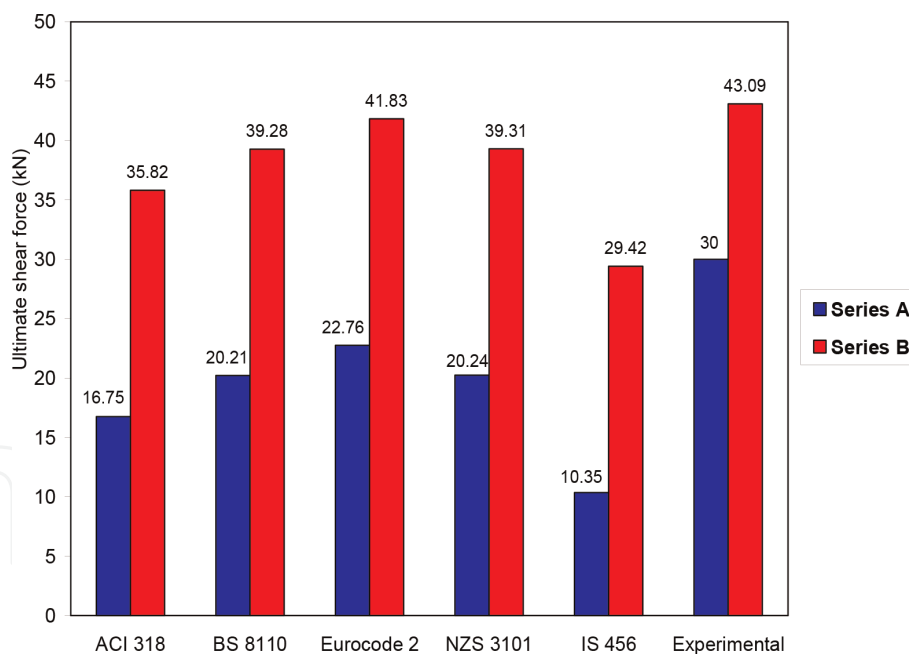


**Figure 17.** Experimental and predicted values of the shear strength of HSC beams.

of HSC material to the shear strength of reinforced concrete beams. An average around 40% of underestimating was recorded. Among the five models, The European Eurocode 2 gives the best predictions with underestimating of around 24% the shear strength of HSC beams. By comparison, the Indian Standard IS456 is the most conservative to predict the ultimate shear force of HSC beams with a prediction of around 65% below the experimental results. This requires more effort and research to extrapolate and to valid these models developed essentially for normal strength concrete to HSC and therefore faithfully reflect the contribution of this new material to the shear strength of reinforced concrete beams.

The Series B of the beams is transversely reinforced by stirrups, the ultimate shear force of this series represents the contribution of concrete ( $V_c$ ) and the contribution of stirrups ( $V_s$ ) to the shear strength of HSC beams. The ultimate shear strength of this series is also shown in **Figure 17**. The concrete contribution  $V_c$  represents 70% of the total shear force and the steel contribution  $V_s$  represents 30%. Therefore, the presence of the transverse reinforcement has improved the ultimate shear strength of HSC beams by around 30%. The five design codes greatly overestimate the contribution of the stirrups to the shear strength of HSC beams. An average overestimation is around 45% was recorded. This is due to the fact that the contribution of the stirrups to the shear strength developed in the five code models is based on the yielding of this reinforcement; this is the Ritter [23] and Mörsh [24] truss analogy. The analogy proposes that a reinforced concrete beam failing after yielding of the transverse reinforcement, and before the crushing of concrete. In all tested beams, the failure mode is characterized by crushing of concrete after the complete penetration of the diagonal cracking in the compression zone of the beam as shown in **Figure 10(b)**, and in the same time the transverse reinforcements have not yielding. The contradiction between the analogy of Ritter and Mörsh and the experimental observations led to a greatly overestimation of the transverse reinforcement contribution to the shear strength of reinforced concrete beams.

On adding up the contribution of concrete and the contribution of the stirrups to the shear strength of HSC beams, Eurocode 2 seems to give the best predictions for the ultimate shear strength compared to other code models.

The five universal design codes require more refinement to reflect the real contributions of both materials; the HSC and the steel reinforcement, to the shear resistance of high strength reinforced concrete beams.

#### 4. Conclusion

A Series of high strength reinforced concrete beams under shear was investigated. The effects of the concrete and the transverse reinforcement on the shear behaviour of the beams were verified. The experimental and the theoretical results led to the following conclusion:

- The HSC is sudden, expressing the brittleness and the low ductility of this material.
- The Series A of beams, without stirrups exhibit a relatively fragile behaviour.
- The addition of the stirrups in the Series B of the HSC beams, improves the ductility of this series. The improvement of the ductility is particularly needed in the regions of higher seismicity to avoid the catastrophic failure of structures.
- The diagonal cracking is efficiently restrained by the stirrups, because their occurrence is delayed and their opening is very fine and did not exceeds the serviceability limit of crack width ( $W_k = 0.3$  mm).
- The digital image correlation technique gives best and very precise results.
- The ultimate shear resistance of HSC beams is increased with the presences of the stirrups. An increase of around 50% was recorded.

- The contribution of the HSC to the shear resistance of reinforced concrete beams was underestimated by the five universal design codes, and in the same time, the contribution of the stirrups was overestimated. These design codes need more refinement to reflect and to ascertain the improved shear strength of high strength reinforced concrete beams.

## Acknowledgements

The experimental investigation presented in this chapter was sponsored by the Ministry of Higher Education and Scientific Research of Algeria. The tests were carried out at Laboratory of Engineering of the Materials of Bretagne (LIMATB) at the University of Bretagne Sud, Lorient, France. Also, Dr. Thibaut Lecompte is gratefully thanked for their willing discussion and active participation in the project.

## Author details


Touhami Tahenni<sup>1\*</sup> and Thibaut Lecompte<sup>2</sup>

1 Department of Technology, Faculty of Sciences and Technology, Djilali Bounaama University of Khemis Miliana, Khemis Miliana, Algeria

2 Université de Bretagne-Sud, Lorient, France

\*Address all correspondence to: [touhami\\_tahenni@yahoo.fr](mailto:touhami_tahenni@yahoo.fr)

## IntechOpen

© 2019 The Author(s). Licensee IntechOpen. This chapter is distributed under the terms of the Creative Commons Attribution License (<http://creativecommons.org/licenses/by/3.0>), which permits unrestricted use, distribution, and reproduction in any medium, provided the original work is properly cited. 



## References

- [1] Pendyala RS, Mendis P. Experimental study on shear strength of high strength concrete beams. *ACI Structural Journal*. 2000;**97**(4):564-571
- [2] Johnson MK, Ramirez JA. Minimum shear reinforcement in beams with higher strength concrete. *ACI Structural Journal*. 1989;**86**(4):376-382
- [3] Cladera A, Mari AR. Experimental study on high-strength concrete beams failing in shear. *Engineering Structures*. 2005;**27**:1519-1527
- [4] Khuntia M, Stojadinovic B. Shear strength of reinforced concrete beams without transverse reinforcement. *ACI Structural Journal*. 2001;**98**(5):648-656
- [5] ACI Committee 318. *Building Code Requirements for Structural Concrete: (ACI 318-02) and Commentary (ACI 318R-02)*. Farmington Hills, MI; 2002. 1414 p
- [6] Tahenni T. Etude de la capacité portante en effort tranchant des poutres en béton armé renforcées en fibres d'acier avec référence particulière aux poutres en béton à hautes performances [Doctoral Thesis]. Algiers, Algeria: University of Science and Technology Houari Boumediene; 2016. 208 p
- [7] Chemrouk M. Selection of the mix constituents to produce a highly performing and durable concrete material. In: Nil Turkery A, Zengul O, editors. *Paper Published in 'Durability of Building Materials and Components: Globality and Locality in Durability'*; Vol. 1. Istanbul. 2008. pp. 25-32. ISBN: 978-975-561-326-0
- [8] Chemrouk M, Hamrat M. High performance concrete-experimental studies of the material. In: *Proceeding of the International Congress. The Challenges of Concrete Construction, Conference 1: Innovation and Development in Concrete*; 2002
- [9] Gutierrez PAA, Canovas MF. High performance concrete: Requirements for constituents materials and mix proportioning. *ACI Materials Journal*. 1996;**93**(3):233-241
- [10] Malier I. *Les Bétons à Haute Performance: Caractéristiques, Durabilité, et Applications*. Paris: Presse de l'Ecole Nationale des Ponts et Chaussée; 1992
- [11] GOM Aramis user manuel. v6. 2007. GOM mbH: Germany. Available from: <http://www.gom.com> [Accessed: 7 March 2019]
- [12] Tahenni T, Chemrouk M, Lecompte T. Effect of steel fibers on the shear behavior of high strength concrete beams. *Construction and Building Materials*. 2016;**105**:14-28
- [13] Tahenni T, Chemrouk M, Lecompte T. Shear behavior of high performance concrete beams using digital image correlation technique. In: *Proceedings of the 4th Congrès International de Géotechnique-Ouvrage-Structures, CIGOS*. 26-27 October 2017; Ho Chi Minh City, Vietnam: *Lecture Notes in Civil Engineering*; Vol. 8. 2018. pp. 560-570. DOI: 10.1007/978-981-10-6713-6\_55
- [14] Hamrat M, Boulekbache B, Chemrouk M, Amziane S. Shear behaviour of RC beams without stirrups made of normal strength and high strength concretes. *Advances in Structural Engineering*. 2010;**13**(1): 29-41
- [15] Hamrat M, Boulekbache B, Chemrouk M, Amziane S. Effects of the transverse reinforcement on the shear behaviour of high strength concrete

beams. *Advances in Structural Engineering*. 2012;**15**(8):1291-1306

[16] Hamrat M. Comportement structurel du béton à hautes performances (flexion et effort tranchant) [Doctoral Thesis]. Algeria: University of Science and Technology Houari Boumediene; 2010. 143 p

[17] Taylor HPJ. The shear strength of large beams. *Proceeding ASCE*. 1972;**98**:2473-2490

[18] Fenwick RC, Paulay T. Mechanisms of shear resistance of concrete beams. *Journal Structure Division-ASCE*. 1968; **94**:2325-2350

[19] BS 8110. *Structural Use of Concrete, Part 1. Code of Practice for Design and Construction*. London: British Standards Institution; 1997. 173 p

[20] Eurocode 2. *Design of Concrete Structures—Part 1-1. General Rules and Rules for Buildings*. EN1992-1-1,R. 2004. 100 p

[21] National Standards of New Zealand. NZS 3101—Part 1. *Concrete Structures Standard*. Wellington, New Zealand: Standards New Zealand; 2006

[22] Indian Standard. IS 456. *Plain an reinforced concrete code of practice. (Fourth Revision)*; 2000. 114 p

[23] Ritter W. *Schweizerische Bauzeitung (Zürich). Die Bauweise Hennebique*. 1899;**33**:59-61

[24] Mörsch E. *Der Eisenbetonbau, seine Anwendung und Theorie*. 3ème ed. New York: McGraw-Hill; 1902